

# RUNX3 levels in human hematopoietic progenitors are regulated by aging and dictate erythroid-myeloid balance

Peter Balogh,<sup>1</sup> Emmalee R. Adelman,<sup>2</sup> John V. Pluvinae,<sup>3</sup> Brian J. Capaldo,<sup>4</sup> Katie C. Freeman,<sup>1</sup> Sandeep Singh,<sup>1</sup> Kamaleldin E. Elagib,<sup>1</sup> Yukio Nakamura,<sup>5</sup> Ryo Kurita,<sup>6</sup> Goro Sashida,<sup>7</sup> Eli R. Zunder,<sup>8</sup> Hui Li,<sup>1</sup> Alejandro A. Gru,<sup>1</sup> Elizabeth A. Price,<sup>9</sup> Stanley L. Schrier,<sup>9</sup> Irving L. Weissman,<sup>10</sup> Maria E. Figueroa,<sup>2</sup> Wendy W. Pang,<sup>11\*</sup> and Adam N. Goldfarb<sup>1\*</sup>

<sup>1</sup>Department of Pathology, University of Virginia School of Medicine, Charlottesville, USA; <sup>2</sup>Sylvester Comprehensive Cancer Center, University of Miami Health System, Miami, Florida, USA; <sup>3</sup>Department of Medicine, Stanford University, Stanford, California, USA; <sup>4</sup>Flow Cytometry Core Facility, University of Virginia School of Medicine, Charlottesville, Virginia, USA; <sup>5</sup>Cell Engineering Division, RIKEN BioResource Center, Tsukuba, Ibaraki, Japan; <sup>6</sup>Research and Development Department, Central Blood Institute, Blood Service Headquarters, Japanese Red Cross Society, Tatsumi, Koto-ku, Tokyo, Japan; <sup>7</sup>Laboratory of Transcriptional Regulation in Leukemogenesis IRCMS, Kumamoto University, Chuo-ku, Kumamoto, Japan; <sup>8</sup>Department of Biomedical Engineering, University of Virginia, Charlottesville, Virginia, USA; <sup>9</sup>Department of Medicine, Division of Hematology, Stanford University, Stanford, California, USA; <sup>10</sup>Institute for Stem Cell Biology and Regenerative Medicine, Stanford University, Stanford, California, USA and <sup>11</sup>Department of Medicine, Division of Blood and Bone Marrow Transplantation, Stanford University, Stanford, California, USA

\*WWP and ANG contributed equally to this work

## ABSTRACT

Healthy bone marrow progenitors yield a co-ordinated balance of hematopoietic lineages. This balance shifts with aging toward enhanced granulopoiesis with diminished erythropoiesis and lymphopoiesis, changes which likely contribute to the development of bone marrow disorders in the elderly. In this study, RUNX3 was identified as a hematopoietic stem and progenitor cell factor whose levels decline with aging in humans and mice. This decline is exaggerated in hematopoietic stem and progenitor cells from subjects diagnosed with unexplained anemia of the elderly. Hematopoietic stem cells from elderly unexplained anemia patients had diminished erythroid but unaffected granulocytic colony forming potential. Knockdown studies revealed human hematopoietic stem and progenitor cells to be strongly influenced by RUNX3 levels, with modest deficiencies abrogating erythroid differentiation at multiple steps while retaining capacity for granulopoiesis. Transcriptome profiling indicated control by RUNX3 of key erythroid transcription factors, including *KLF1* and *GATA1*. These findings thus implicate RUNX3 as a participant in hematopoietic stem and progenitor cell aging, and a key determinant of erythroid-myeloid lineage balance.

## Introduction

Hematopoietic stem and progenitor cells (HSPC) execute tightly co-ordinated self-renewal and lineage commitment programs that generate a balanced output of peripheral blood cell types. With aging, these programs undergo perturbation resulting in increased numbers and decreased function within the stem cell compartment as well as a shift in the balance of cell types produced – namely, an increased proportion of granulocytes at the expense of erythroid and lymphoid lineages.<sup>1-4</sup> Thus normal aged mice have diminished peripheral red blood cells and lymphocytes, increased circulating neutrophils and monocytes, and increased sensitivity to granulocyte-colony stimulating factor (G-CSF)-induced leukocytosis and HSPC mobilization.<sup>5,6</sup> The transplantability of age-related HSPC changes highlights



Haematologica 2020  
Volume 105(4):905-913

## Correspondence:

ADAM N. GOLDFARB  
ang3x@virginia.edu

Received: October 19, 2018.

Accepted: June 5, 2019.

Pre-published: June 6, 2019.

doi:10.3324/haematol.2018.208918

Check the online version for the most updated information on this article, online supplements, and information on authorship & disclosures: [www.haematologica.org/content/105/4/905](http://www.haematologica.org/content/105/4/905)

©2020 Ferrata Storti Foundation

Material published in *Haematologica* is covered by copyright. All rights are reserved to the Ferrata Storti Foundation. Use of published material is allowed under the following terms and conditions:

<https://creativecommons.org/licenses/by-nc/4.0/legalcode>.

Copies of published material are allowed for personal or internal use. Sharing published material for non-commercial purposes is subject to the following conditions:

<https://creativecommons.org/licenses/by-nc/4.0/legalcode>, sect. 3. Reproducing and sharing published material for commercial purposes is not allowed without permission in writing from the publisher.



the importance of cell-intrinsic determinants, although micro-environmental factors also exert a critical influence.<sup>7-9</sup>

The transcription factor *RUNX3* has been characterized as a participant in neural and lymphocyte development, TGF $\beta$  signaling, and solid tumor suppression.<sup>10-14</sup> Several studies have also demonstrated its repression in aged normal as well as tumor tissues, with the principal mechanism of inactivation being epigenetic alterations, particularly DNA methylation.<sup>15-18</sup> Emerging data suggest a role in hematopoiesis, with zebrafish and murine loss of function studies revealing progenitor perturbations, although the extent of its role has remained unclear due to redundancy with *Runx1*.<sup>19-21</sup> Most notably, induction of hematopoietic *Runx3* deletion in mice elicited marrow changes similar to those reported with normal aging: increased marrow colony forming units (CFU) and increased peripheral blood mobilization of CFU by G-CSF treatment.<sup>5,22</sup>

This study shows *RUNX3* to be expressed in murine and human HSPC, where it undergoes repression and epigenetic modification during normal aging. HSPC levels of *RUNX3* were found to determine developmental potential, with deficiency restricting erythropoiesis at commitment and subsequent stages while fully permitting granulopoiesis. HSPC purified from patients with unexplained anemia of aging manifested *RUNX3* deficiency and similar developmental alterations. Changes in HSPC transcriptome due to *RUNX3* deficiency suggest a role upstream of the erythroid master regulatory transcription factors KLF1 and GATA1.

## Methods

### Cell culture

Human CD34<sup>+</sup> expansion medium consisted of Iscove's modified Dulbecco's medium (IMDM) supplemented with bovine serum albumin, insulin and transferrin (BIT) 9500, and 100 ng/mL each of rhTPO, rhSCF, and rhFlt3-L, plus 10 ng/ml rhIL-3. Erythroid medium consisted of IMDM supplemented with BIT 9500, and 4.5 U/mL rhEPO and 25 ng/mL rhSCF. Megakaryocyte medium consisted of IMDM supplemented with BIT 9500, and 40 ng/mL rhTPO, 25 ng/mL rhSCF, and 20 ng/mL rhSDF1- $\alpha$ . Granulocyte medium consisted of IMDM supplemented with BIT 9500, and 25 ng/mL rhSCF, 10 ng/mL rhIL-3, and 20 ng/mL rhG-CSF. Colony formation assays were conducted using methylcellulose supplemented with 50 ng/mL rhSCF, 10 ng/mL rhIL-3, 20 ng/mL rhIL-6, 3 U/mL rhEPO, 20 ng/mL rhG-CSF, and 10 ng/mL rhGM-CSF.

### Mass cytometry

Cells were stained for viability with 100  $\mu$ M cisplatin, fixed with 1.6% paraformaldehyde, and stored at -80°C. Thawed samples were barcoded, pooled, and surface stained at room temperature for 30 minutes (min). Cells were then permeabilized with methanol and stained for intercellular antigens for 1 hour (h) at room temperature. Next, cells were incubated with Fluidigm CellID Ir-Intercalator, re-suspended in water with normalization beads, and analyzed on a Fluidigm CyTOF 2. Data were bead-normalized and underwent barcode deconvolution using the debarcoding tool MATLAB standalone executable.<sup>23</sup>

Data were inverse hyperbolic sine-transformed using a co-factor of 0.25. FlowSOM was used to construct a self-organizing map, and each cell was assigned a phenocode for every lineage

marker using flowType. Each grid point was then immunophenotyped, and cell counts were tabulated to form a hierarchical count table. Differential abundance was tested for using edgeR with a quasi-likelihood framework as specified by the cydar<sup>TM</sup> package.

### RNA-sequencing

RNA was extracted using the QIAgen RNeasy Plus Mini Kit, with added DNA digestion. Samples underwent ribosomal reduction, and sequencing with 100bp, paired-end, and 50 million read-depth parameters on an Illumina HiSeq 2500 machine. Data were processed online at usegalaxy.org. Trimmomatic was used to eliminate low quality sequences from the reads, followed by alignment to the hg19 reference genome using HISAT2, and RmDup to eliminate PCR duplicates. Differential gene expression was assessed with both DESeq2 and Cufflinks tools. The Synergizer tool was used to convert UCSC gene identifiers into hgnc gene symbols.

### Unexplained anemia of the elderly studies

Mononuclear cells were sorted phenotypically: HSC, Lin<sup>-</sup>CD34<sup>+</sup>CD38<sup>-</sup>CD904<sup>+</sup>CD45RA<sup>-</sup>; MEP, Lin<sup>-</sup>CD34<sup>+</sup>CD38<sup>+</sup>CD123<sup>-</sup>CD45RA<sup>-</sup>. Colony assays were performed using complete methylcellulose with 12-14 days incubation. For microarray, RNA samples were quantified, subjected to reverse transcription, underwent two rounds of linear amplification, and biotinylated. 15  $\mu$ g of RNA per sample was assayed using Affymetrix HG U133 Plus 2.0 microarrays. Data were analyzed using the gene expression commons platform.

### Ethics statement

This study was reviewed and approved by the institutional review boards of the respective institutions and was conducted in accordance with the principles of the Declaration of Helsinki.

### Data and software availability

RNA-sequencing accession numbers: GSE119264, GSE104406. Microarray accession number: GSE123991.

## Results

### Hematopoietic stem cell *RUNX3* levels decline with aging

Prior reports have shown marrow-specific *Runx3* knockout to elicit aspects of the aging phenotype and to exaggerate the myeloid skewing associated with aging.<sup>5,22</sup> We therefore assessed *RUNX3* expression in rigorously purified human and murine hematopoietic stem cells. In humans, RNA-seq has been conducted on Lin<sup>-</sup>CD34<sup>+</sup>CD38<sup>-</sup> marrow cells from healthy young (18-30 years old) and aged (65-75) subjects (GSE104406). In mice, side population (SP) Lin<sup>-</sup>Sca<sup>+</sup>Kit<sup>+</sup>CD150<sup>+</sup> marrow cells from young (4 months old) and aged (24 months) animals have undergone RNA-seq (GSE47819). Both datasets demonstrated HSC expression of *RUNX3* with significant decreases associated with aging (Figure 1A and B). Human CD34<sup>+</sup>CD38<sup>+</sup> later stage progenitors also showed diminished *RUNX3* expression with aging, indicating that the changes are not HSC-restricted (Online Supplementary Figure S1A). Evidence for an aging-associated decline in progenitor protein levels was seen in human marrow samples immunostained for *RUNX3* (Online Supplementary Figure S1B). Analysis of murine bone marrow single-cell RNA-seq datasets<sup>24</sup> (GSE89754) from animals with or without erythropoietin (EPO) treatment confirmed that

the signals for *Runx3* expression came from multipotent and early committed erythroid progenitors rather than contaminant lymphocytes. Discrimination of HSC *versus* MPP compartments is not possible by this approach (Online Supplementary Figure S1C).

Because epigenetic changes occur with HSC aging and

participate in regulation of *RUNX3*,<sup>25-27</sup> we investigated the effect of aging on DNA and histone modifications within the murine and human loci. Analysis of comprehensive DNA methylation mapping by whole genome bisulfite sequencing<sup>3</sup> (GSE47819) revealed significant increases in P2 promoter methylation in aged murine HSC (Figure 1C

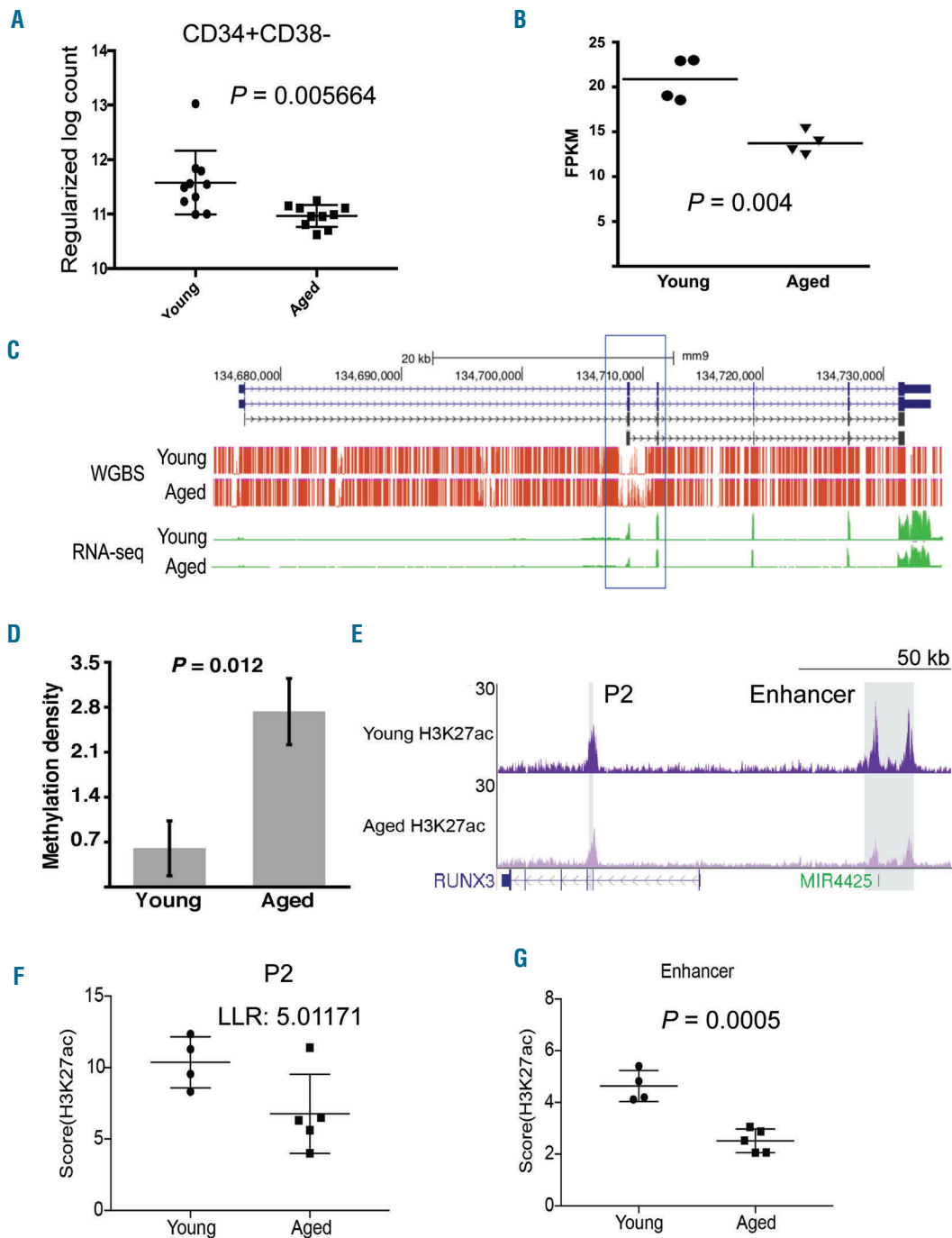


**Figure 1. Hematopoietic stem and progenitor cells (HSPC) and SPC *RUNX3* levels decline with aging.** (A) Human *RUNX3* mRNA levels in Lin<sup>-</sup>CD34<sup>+</sup>CD38<sup>-</sup> bone marrow (BM) HSPC obtained from healthy young and aged individuals. N=10 per group. (B) Mouse *Runx3* mRNA levels in side population, Lin<sup>-</sup>Sca1<sup>+</sup>Kit<sup>+</sup>CD150<sup>-</sup> BM HSC obtained from healthy young and aged animals (GSE478193). N=4 per group. (C and D) Tracks for DNA methylation by whole genome bisulfite sequencing (WGBS, red) and RNA-seq read counts (green) within the mouse *Runx3* locus in HSC from healthy young and aged animals (GSE47819<sup>3</sup>). The blue box highlights the DNA methylation trough associated with the P2 promoter. (D) Mean methylation density (% of CpG reads with methylation) within trough. N=5-6 per group. (E-G) Histone H3K27 acetylation by chromatin immunoprecipitation (ChIP)-sequencing within the human locus in HSPC from healthy young and aged individuals. Gray shading highlights peaks within the P2 promoter and upstream super-enhancer. (F) H3K27ac score for the P2 promoter peak, and (G) the sum of peak scores across the enhancer. N=4-5 per group. All statistics two-tailed Student *t*-test, except in F: log likelihood ratio (LLR). Error bars+standard error of mean. FPKM: fragments per kilobase of transcript per million.

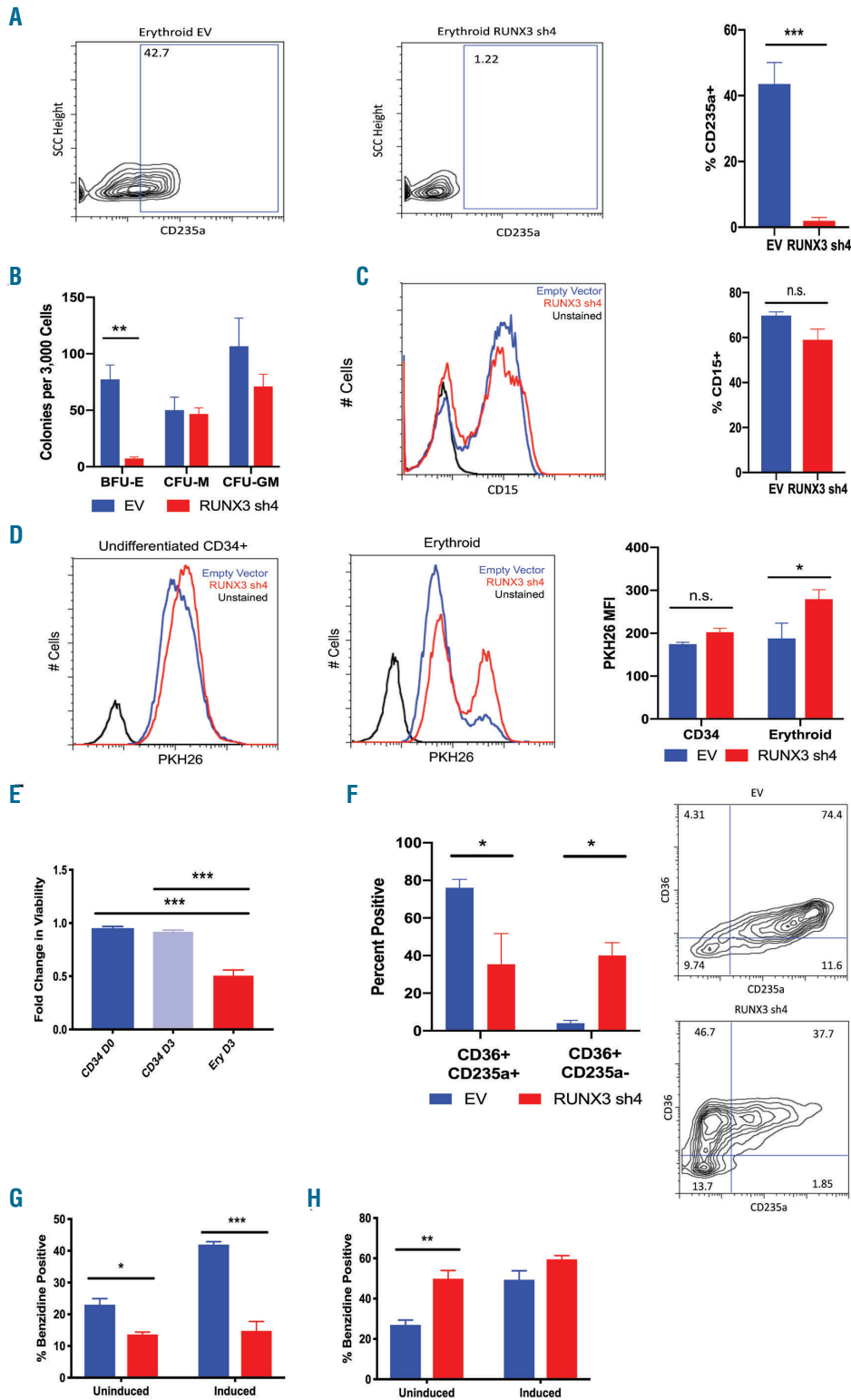


**Figure 2. RUNX3 participates in erythroid but not granulocytic differentiation of human progenitors.** (A) Flow cytometry plots for erythroid differentiation of CD34<sup>+</sup> cells transduced with empty vector (EV) or RUNX3-targeting (RUNX3 sh4) lentiviral shRNA constructs and subjected to unilineage erythroid culture for three days. Graph summarizes the quantitation of erythroid differentiation from three independent experiments. (B) Summary of colony formation assays on CD34<sup>+</sup> cells transduced as in (A). (C) Flow cytometry histogram overlays for granulocyte differentiation of CD34<sup>+</sup> cells transduced as in (A) and subjected to unilineage granulocytic culture for eight days. Representative results from three independent experiments. (D) Flow cytometry histogram overlays for cell proliferation by dye dilution. Transduced CD34<sup>+</sup> cells were stained with PKH26 followed by three days of culture in expansion medium (CD34) or erythroid medium. Graph summarizes mean fluorescence intensity due to dye retention from three independent experiments. (E) Summary of viability as assessed by flow cytometry on CD34<sup>+</sup> cells transduced as in (A) and cultured in expansion or erythroid medium for indicated days. (F) Flow cytometry plots for erythroid differentiation of CD36<sup>+</sup> CD235a<sup>-</sup> early committed erythroid progenitors transduced as in (A) and cultured in erythroid medium for three days. Graph summarizes quantitation of erythroid differentiation from three independent experiments. (G and H) Summary of hemoglobinization, i.e. percent cells positive for benzidine staining, in HUDEP-2 cells transduced with control vectors (EV), RUNX3-knockdown lentivirus (sh4), or RUNX3-overexpression retrovirus (OE). Cells were cultured 48 hours in HUDEP-2 expansion (Uninduced) or differentiation (Induced) medium. N=3. (A and C) Two-tailed Student t-test. (B, D, and F-H) Two-way ANOVA with Bonferroni's test. (E) One-way ANOVA with Tukey's test. \**P*<0.05; \*\**P*<0.01; \*\*\**P*<0.005. Error bars+standard error of mean.

and D). Datasets for H3K27ac in young *versus* aged murine HSC are not currently available. The human RUNX3 locus showed aging-associated decreases in H3K27ac within the P2 promoter, as well as the super-enhancer region located approximately 97 kilobases upstream of the P2 promoter-28 (GSE104406) (Figure 1E-G).

**RUNX3 in human hematopoietic stem and progenitor cells participates in erythroid programming**

The decline in HSC RUNX3 levels with aging illustrated in Figure 1A raised questions about potential roles in human hematopoietic differentiation. Human CD34<sup>+</sup> HSPC cultures were used to examine protein expression

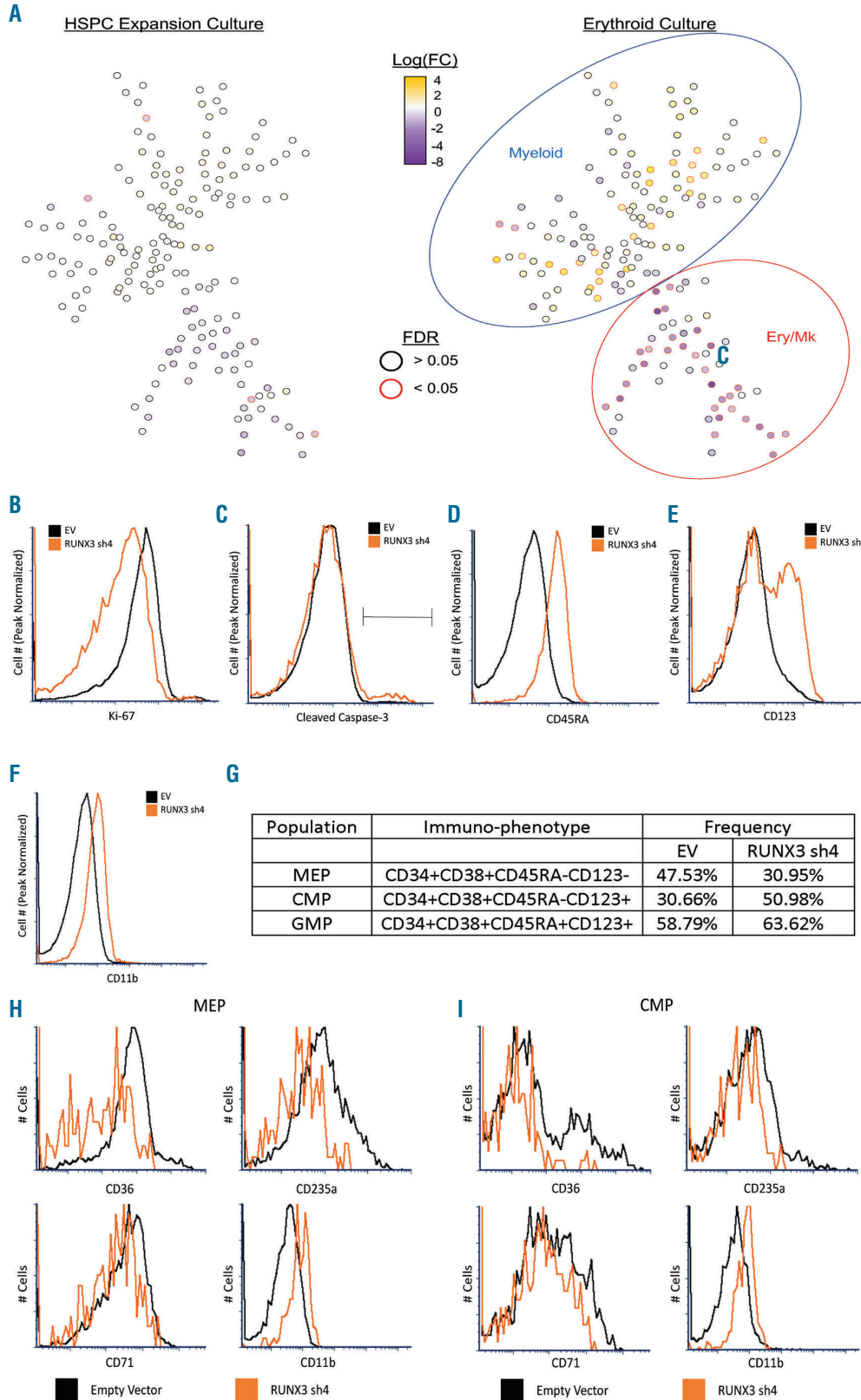


**Figure 3. RUNX3 levels influence progenitor lineage output balance.** (A) Minimum spanning tree plots depicting cell population-nodes identified by cytometry on a Fluidigm CyTOF 2 on indicated cultures of transduced CD34<sup>+</sup> progenitors. Heatmap coloration of nodes reflects log<sub>2</sub>(fold changes) in their frequency associated with RUNX3 knockdown. Erythroid-megakaryocytic (Ery/Mk) and myeloid compartments are indicated by red and blue ovals, respectively. (B and C) CyTOF histogram overlays from transduced progenitors cultured in erythroid medium, comparing expression of Ki-67 and cleaved caspase-3 between control (EV, black) and RUNX3-deficient (RUNX3 sh4, orange) populations in the Ery/Mk compartment. (D-F) CyTOF histogram overlays from transduced progenitors cultured in erythroid medium, comparing expression of CD123, CD45RA, and CD11b between control (EV, black) and RUNX3-deficient (RUNX3 sh4, orange) populations in the Ery/Mk compartment. (G) Frequencies of megakaryocyte-erythroid progenitors (MEP), common myeloid progenitors (CMP), and granulocyte-monocyte progenitor (GMP) populations calculated from all cells cultured in erythroid medium. (H and I) Histogram overlays comparing CD36, CD235a, CD71, and CD11b expression between control (EV, black) and RUNX3-deficient (RUNX3 sh4, orange) MEP and CMP.

and function. By immunoblot, the initial undifferentiated population displayed relatively high *RUNX3* levels, with a gradual decline occurring during erythroid differentiation (Online Supplementary Figure S2A). Immunofluorescent staining revealed predominantly cytoplasmic localization in the undifferentiated cells and enhanced nuclear localization associated with erythroid differentiation (Online Supplementary Figure S3). Transduction of HSPC with empty or *RUNX3*-targeting lentiviral shRNA vectors did not alter the localization of *RUNX3* in erythroid differentiated cells. Both nuclear and cytoplasmic patterns of *RUNX3* localization have been observed in prior studies, and may reflect SMAD or STAT activation status as previously described.<sup>29-32</sup>

Partial knockdown of *RUNX3* with three independent lentiviral short RNA hairpins blocked erythroid differentiation of CD34<sup>+</sup> progenitors, preventing expression of glycoprotein A (CD235a) (Figure 2A and Online Supplementary Figure S2B). Subsequent experiments employed short hairpin #4 due to robust knockdown (approx. 60% protein loss) with no significant cross-inhibition of other *RUNX* proteins (Online Supplementary Figure S2C). As additional controls, CD34<sup>+</sup> progenitors also underwent transduction with shRNA vectors targeting GFP, which had no effect on erythroid differentiation, and *RUNX1*, which slightly enhanced erythroid differentiation as described<sup>33</sup> (Online

Supplementary Figure S2D and E). *RUNX3* deficiency in CD34<sup>+</sup> HSPC also blocked erythroid colony formation in semi-solid medium, with no significant impact on mono-cyte or mixed granulocyte-monocyte colonies (Figure 2B). As with the colony assays, *RUNX3* deficiency caused minimal changes in granulocyte differentiation (CD15) after eight days of suspension culture (Figure 2C). When maintained in uni-lineage, serum-free erythroid medium containing EPO and stem cell factor (SCF), *RUNX3*-deficient progenitors showed time-dependent declines in proliferation and viability (Figure 2D and E). By contrast, *RUNX3*-deficient progenitors cultured in expansion medium with SCF, IL-3, thrombopoietin (TPO), and Flt3-ligand retained normal proliferation and near-normal viability (Figure 2D and E). However, *RUNX3* knockdown did prevent HSPC upregulation of CD41 in megakaryocytic cultures, suggesting an influence at the level of erythro-megakaryocytic progenitors (Online Supplementary Figure S2F).

To determine contributions to post-commitment human erythropoiesis, we knocked down *RUNX3* in sorted CD36<sup>+</sup>CD235a<sup>-</sup> early erythroid progenitors. *RUNX3* deficiency in these cells impaired their progression to the more mature CD36<sup>+</sup>CD235a<sup>+</sup> stage, indicating involvement in post-commitment differentiation (Figure 2F). Knockdown of *RUNX3* in the human HUDEP-2 pro-ery-

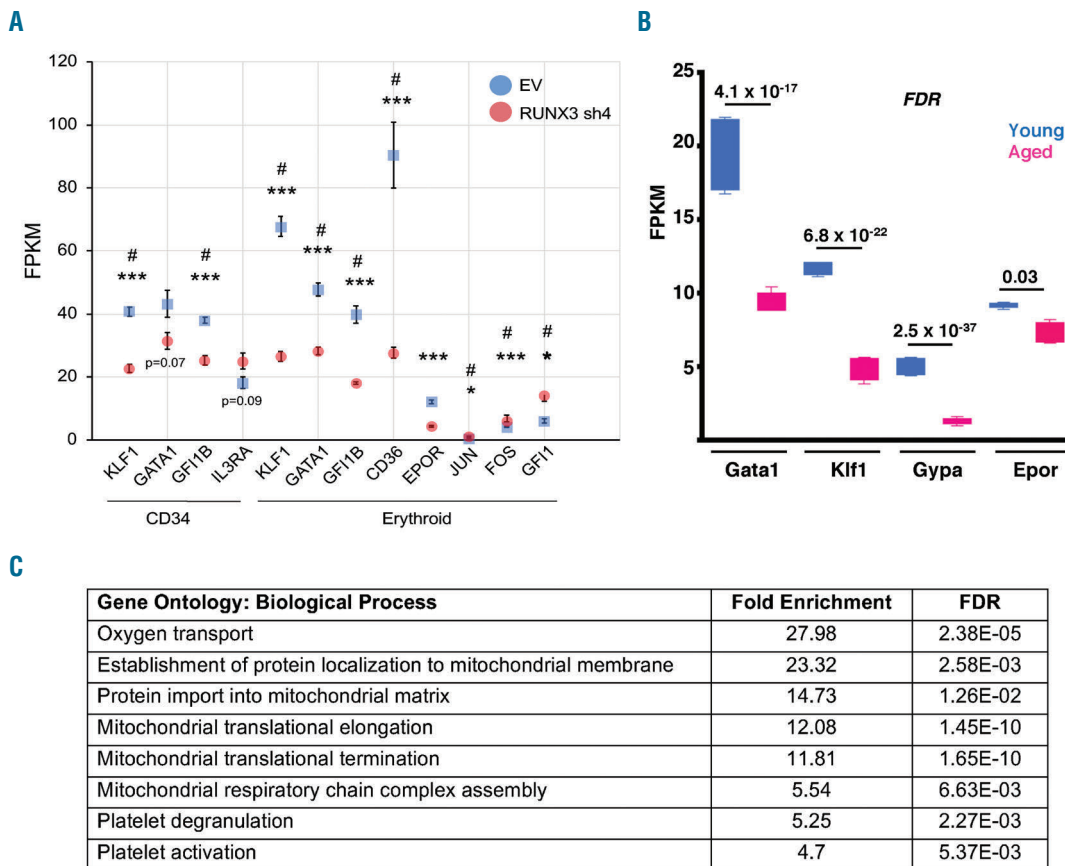


Figure 4. *RUNX3* deficiency causes perturbations in erythroid transcriptional program. (A) Fragments per kilobase of transcript per million (FPKM) read counts of relevant genes in transduced progenitors cultured in expansion or erythroid medium. N=3. (B) FPKM read counts of key erythroid genes in young and aged murine hematopoietic stem cells (HSC) as in Figure 1B (GSE478193). (C) Gene Ontology classification by biological process of gene sets significantly down-regulated in association with *RUNX3* deficiency in cells undergoing erythroid culture. N=3. All statistics False Discovery Rate (FDR), denoted by '#' in (A) (DESeq2), plus two-tailed Student t-test for FPKM values denoted by asterisks in (A). \*P<0.05; \*\*P<0.01; \*\*\*P<0.005. Error bars±standard error of mean. EV: control vectors.

throblast line shifted the cells to a less mature phenotype, characterized by increased CD71 and diminished CD235a expression, and blocked induction of hemoglobinization (Figure 2G and *Online Supplementary Figure S2G-I*). Conversely, retroviral overexpression of RUNX3 in HUDEP-2 pro-erythroblasts enhanced their hemoglobinization (Figure 2H and *Online Supplementary Figure S2I*).

### Progenitor deficiency of RUNX3 alters the balance of lineage output

To analyze in greater detail the effects of RUNX3 deficiency on progenitor fates, mass cytometry (CyTOF) was employed for comprehensive single cell profiling of cells in HSPC expansion culture, and cells in erythroid, megakaryocyte, or granulocyte culture conditions for 48 h. Cells from each culture condition were clustered into populations defined by surface marker staining, followed by construction of minimum spanning tree (MST) plots describing average fold changes in population abundance associated with RUNX3 knockdown (Figure 3A and *Online Supplementary Figure S4A and B*). These populations segregated into two main branches: a lower erythromegakaryocytic compartment (Ery/Mk: red oval) defined by CD36 and/or CD41 positivity, and an upper compartment (Myeloid: blue oval) lacking both markers (*Online Supplementary Figure S4C and D*). As expected from results in Figure 2, RUNX3 knockdown selectively diminished cell populations within the Ery/Mk compartment in lineage culture conditions, but not in HSPC expansion conditions (Figure 3A and *Online Supplementary Figure S4A*). This contraction was associated with impaired proliferation, as reflected by decreased Ki-67 expression, but with no evidence of increased apoptosis (Figure 3B and C).

Notably, populations in the myeloid compartment (blue oval) were augmented in RUNX3-deficient progenitors grown in erythroid medium but not in other culture conditions. Analysis of these populations revealed a myeloid-skewed shift in HSPC distribution, similar to what has been described in aged bone marrow. These populations displayed a GMP (granulocyte-monocyte progenitor) phenotype, based on expression of CD34, CD38, CD123, and CD45RA in various combinations (*Online Supplementary Table S1*). Strikingly, RUNX3-deficient populations in the Ery/Mk compartment (red oval) exhibited aberrant retention of CD123, as well as global upregulation of the GMP marker CD45RA and the myeloid differentiation antigen CD11b (Figure 3D-F).

The CyTOF panel permitted assessment of the frequencies of cells with marker profiles of megakaryocyte-erythroid progenitors (MEP), common myeloid progenitors (CMP), and granulocyte monocyte progenitors (GMP).<sup>34</sup> This analysis showed RUNX3 deficiency to decrease MEP frequency and increase CMP and GMP frequencies (Figure 3G and *Online Supplementary Figure S4E*). Within the CMP and MEP compartments, knockdown of RUNX3 was associated with diminished expression of erythroid markers CD36 and CD235a, but enhanced expression of the myeloid marker CD11b (Figure 3H and I and *Online Supplementary Figure S4F*).

### RUNX3 deficiency causes perturbations in erythroid transcriptional program

To identify the genes affected by RUNX3 knockdown, we performed mRNA sequencing on undifferentiated

CD34<sup>+</sup> cells and cells in erythroid culture for 24 h, before cell viability was impacted by RUNX3 deficiency. In line with our other data, few changes were found between control and RUNX3-deficient undifferentiated cells (<70 genes with differential expression). However, among the down-regulated genes were key erythroid transcription factors including *KLF1*, *GATA1*, and *GFI1B* (Figure 4A). Several globin- and erythroid blood group antigen-encoding genes were decreased as well (*data not shown*). Notably, *Klf1*, *Gata1*, and downstream erythroid target genes *Gypa* and *Epor* also underwent downregulation in aged *versus* young murine HSC (Figure 4B). When comparing control and RUNX3-deficient progenitors in erythroid culture, approximately 1,100 genes showed differential expression. These included many of the same genes affected in the undifferentiated cells as well as additional erythroid genes such as CD36 and EPOR (Figure 4A). In addition, several granulocytic transcription factors were aberrantly up-regulated, including *GFI1*, *JUN*, and *FOS* (Figure 4A). Gene ontology (GO) analysis of genes differentially expressed in control *versus* RUNX3-deficient undifferentiated progenitors revealed only two significant functional categories, oxygen transport (i.e. erythroid; >100-fold enrichment; FDR 1.22E-6) and blood coagulation (i.e. megakaryocytic; 15.08-fold enrichment; FDR 1.91E-3), both of which showed downregulation. GO analysis of progenitors in erythroid culture yielded similar results but also included genes related to mitochondrial protein synthesis/transport and ribosomal biogenesis (Figure 4C).

### Hematopoietic stem and progenitor cells RUNX3 deficiency occurs in human anemias associated with aging

Because RUNX3 expression levels strongly influence human erythroid differentiation, its downregulation could potentially contribute to anemias associated with aging. To address this possibility, we analyzed highly purified marrow progenitors from the following subjects: normal non-anemic young (20-35 years old), non-anemic aged (>65 years old), and aged (>65 years old) subjects with unexplained anemia of the elderly (UAE). The diagnosis of UAE was made by ruling out all other potential causes of anemia, as per the criteria of Goodnough and Schrier.<sup>35</sup> Gene expression profiling by microarray confirmed RUNX3 downregulation in UAE *versus* aged HSC4 (GSE32719) (Figure 5A). Functional studies revealed intrinsic differences in lineage output between UAE and non-anemic old progenitors. UAE HSC yielded fewer erythroid colonies (BFU-E) but similar numbers of myeloid colonies (CFU-GM) (Figure 5B). These findings resemble the effects of RUNX3 knockdown on colony formation by CD34<sup>+</sup> progenitors (Figure 2B). Furthermore, UAE MEP also showed poor TGF $\beta$  responsiveness in erythroid colony (CFU-E) enhancement (Figure 5C), a notable finding given the known influences of HSC aging and RUNX3 expression on this pathway.<sup>3,36</sup>

### Discussion

Hematopoietic stem cell alterations with aging are complex; they result from cell-autonomous and micro-environmental mechanisms, and involve transcriptional changes in numerous genes. Interestingly, several of the

transcriptional programs affected have been previously linked to RUNX3 function, including quiescence, DNA-damage responsiveness, and TGF $\beta$  signaling.<sup>12,20,26,36,37</sup> Decreased *RUNX3* in aged tissues has been previously reported but was analyzed in heterogeneous mixtures of mature cell types.<sup>15-18</sup> Our results derive from purified, long-lived stem cells and reveal conservation between mice and humans. The repressive mechanism likely relates to the aging-associated epigenetic changes identified. Beerman *et al.* have shown that murine HSC aging and proliferative stress reconfigure the DNA methylation landscape, with key erythroid and lymphoid regions targeted for hyper-methylation and repression.<sup>6</sup> The increased *Runx3* P2 promoter methylation we identified in aged murine HSC has also been found in aging of other tissues and cancers.<sup>16,27,38</sup> The aging-associated decreases in H3K27ac that we identified at the human *RUNX3* promoter and upstream super-enhancer may contribute to its repression in human HSC.

A feature of HSC aging conserved from mice to humans consists of myeloid skewing characterized by augmented marrow production of neutrophils and monocytes at the expense of erythroid and lymphoid cells.<sup>1-3</sup> *RUNX3* deficiency in aged mice likewise yields increased myelopoiesis; however, it presents as a myeloproliferative disorder, which appears to be distinct from age-associated myeloid skewing due to lack of B-cell and T-cell perturbations, and a relatively mild erythroid deficit that may be secondary to leukocytosis.<sup>22</sup> Despite these differ-

ences, our study indicates that loss of *RUNX3* diminishes the expression of genes required for the erythroid program, and potentially de-represses myeloid genes. Epigenetic and transcriptomic analysis of aged HSC have also indicated that myeloid-skewing may manifest after similar changes.<sup>6,7</sup> Other aging-like phenotypes of *RUNX3* deficiency include expansion of the LSK<sup>+</sup> HSPC compartment, and increased HSPC mobilization in response to G-CSF.<sup>22</sup> Thus, loss of *RUNX3* contributes to age-associated HSPC phenotypes, although likely cooperates with other perturbations to generate *bona fide* myeloid-skewing.

Additional studies have implicated *RUNX3* in non-lymphoid hematopoietic development. In human CD34<sup>+</sup> cell erythroid cultures, *RUNX3* was predicted by Cytoscape MiMI analysis of gene expression profiles to be a “parent protein,” i.e. a central node, in an erythroid transcription factor network.<sup>39</sup> In zebrafish, morpholino knockdown of *runx3* during embryogenesis resulted in severe anemia.<sup>19</sup> Our results define a novel role for *RUNX3* in the erythropoietic program, governing the expression of lineage-specific transcription factors such as *KLF1*, *GATA1*, and *GFI1B*. Notably, *Klf1* and *Gata1* displayed downregulation in aged murine HSC. We further show that *RUNX3* deficiency produces perturbations at multiple developmental stages including MEP and committed erythroid progenitors. The decreased proliferation seen in *RUNX3*-deficient progenitors may contribute to differentiation impairment. However, the retained capacity for myeloid differentiation

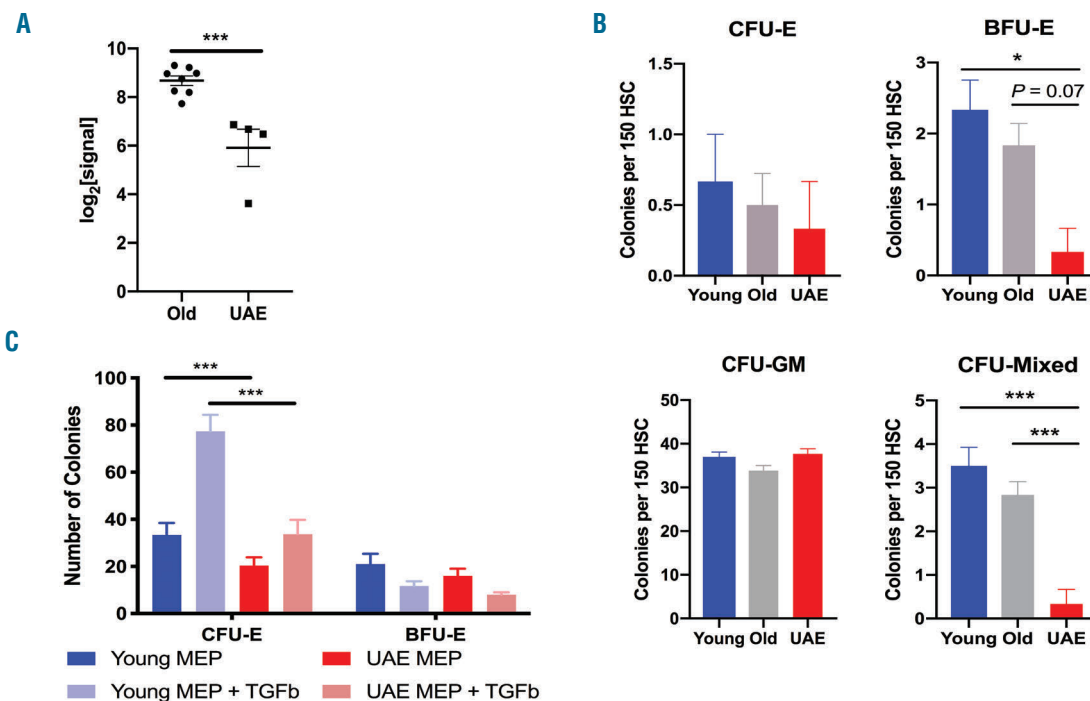


**Figure 5. Decreased *RUNX3* expression and impaired erythropoiesis in unexplained anemia of the elderly.** (A) Log<sub>2</sub>[signal] derived from microarray analysis of *RUNX3* mRNA levels in purified human marrow hematopoietic stem cells (HSC) and common myeloid progenitors (CMP) from normal old and unexplained anemia of the elderly (UAE) subjects. N=4-8 per group. (B) Summary of colony formation assays on 150 HSC from normal young, normal old, and UAE subjects. N=3-6 per group. (C) Summary of erythroid colony formation assays  $\pm$  TGF $\beta$  on 150 megakaryocyte-erythroid progenitors (MEP) from normal young versus UAE subjects. (A) Two-tailed Student *t*-test. (B) One-way ANOVA with Tukey's Test. (C) Two-way ANOVA with Bonferroni's test. \**P*≤0.05; \*\**P*≤0.01; \*\*\**P*≤0.005. Error bars+standard error of mean. CFU-E: colony forming unit erythroid; BFU-E: burst forming unit erythroid; CFU-GM: granulocyte-macrophage progenitor.



and the aberrant retention of GMP markers such as CD123 and CD45RA on RUNX3 deficient cells suggests an additional role in lineage resolution. Taken together, the current findings implicate RUNX3 in the maintenance of bone marrow lineage balance and identify its decline in aged HSPC as a likely contributory factor in aging-associated anemias.

### Acknowledgments

Thank you to Nicole Brimer for providing the packaging plasmids for production of retroviral particles. Thank you to Joanne Lannigan, Michael Solga, Claude Chew, Alexander Wendling, and Lesa Campbell for assistance with flow cytometry experi-

ments at the University of Virginia Flow Core Facility. Thank you to Pat Pramoojago and Rebecca Blackwell for assistance with immunohistochemistry experiments at the Biorepository and Tissue Research Facility. Thank you to Janet Cross, Michael McConnell, John Bushweller and Mazhar Adli for project guidance and discussion.

### Funding

This work was funded by the following NIH grants: R01 HL130550, R01 DK079924, R01 DK101550. PB was supported in part by grant NIH T32 CA009109-39 (Cancer Research Training in Molecular Biology) awarded to the University of Virginia.

### References

- Choudry FA, Frontini M. Epigenetic Control of Haematopoietic Stem Cell Aging and Its Clinical Implications. *Stem Cells Int.* 2016;2016:5797521.
- Akunuru S, Geiger H. Aging, Clonality and Rejuvenation of Hematopoietic Stem Cells. *Trends Mol Med.* 2016;22(8):701-712.
- Sun D, Luo M, Jeong M, et al. Epigenomic profiling of young and aged HSCs reveals concerted changes during aging that reinforce self-renewal. *Cell Stem Cell.* 2014;14(5):673-688.
- Pang WW, Price E a, Sahoo D, et al. Human bone marrow hematopoietic stem cells are increased in frequency and myeloid-biased with age. *Proc Natl Acad Sci.* 2011;108(50):20012-20017.
- Xing Z, Ryan MA, Daria D, et al. Increased hematopoietic stem cell mobilization in aged mice. *Blood.* 2012;108(7):2190-2197.
- Beerman I, Bock C, Garrison BS, et al. Proliferation-dependent alterations of the DNA methylation landscape underlie hematopoietic stem cell aging. *Cell Stem Cell.* 2013;12(4):413-425.
- Rossi DJ, Bryder D, Zahn JM, et al. Cell intrinsic alterations underlie hematopoietic stem cell aging. *Proc Natl Acad Sci U S A.* 2005;102(26):9194-9199.
- Yamamoto R, Wilkinson AC, Ooehara J, et al. Large-Scale Clonal Analysis Resolves Aging of the Mouse Hematopoietic Stem Cell Compartment. *Cell Stem Cell.* 2018;22(4):600-607.
- Maryanovich M, Zahalka AH, Pierce H, et al. Adrenergic nerve degeneration in bone marrow drives aging of the hematopoietic stem cell niche. *Nat Med.* 2018;24(6):782-791.
- Chi XZ, Lee JW, Lee YS, Park IY, Ito Y, Bae SC. Runx3 plays a critical role in restriction-point and defense against cellular transformation. *Oncogene.* 2017;36(50):6884-6894.
- Krishnan V, Chong YL, Tan TZ, et al. TGF promotes genomic instability after loss of RUNX3. *Cancer Res.* 2018;78(1):88-102.
- Fainaru O, Woolf E, Lotem J, et al. Runx3 regulates mouse TGF- $\beta$ -mediated dendritic cell function and its absence results in airway inflammation. *EMBO J.* 2004;23(4):969-979.
- Ebihara T, Song C, Ryu SH, et al. Runx3 specifies lineage commitment of innate lymphoid cells. *Nat Immunol.* 2015;16(11):1124-1133.
- Inoue KI, Shiga T, Ito Y. Runx transcription factors in neuronal development. *Neural Dev.* 2008;3(1):1-7.
- Meng G, Zhong X, Mei H. A systematic investigation into Aging Related Genes in Brain and Their Relationship with Alzheimer's Disease. *PLoS One.* 2016;11(3):1-17.
- So K, Tamura G, Honda T, et al. Multiple tumor suppressor genes are increasingly methylated with age in non-neoplastic gastric epithelia. *Cancer Sci.* 2006;97(11):1155-1158.
- Tserel L, Kolde R, Limbach M, et al. Age-related profiling of DNA methylation in CD8+ T cells reveals changes in immune response and transcriptional regulator genes. *Sci Rep.* 2015;5:13107.
- Wolff EM, Liang G, Cortez CC, et al. RUNX3 methylation reveals that bladder tumors are older in patients with a history of smoking. *Cancer Res.* 2008;68(15):6208-6214.
- Kalev-Zylinska ML, Horsfield JA, Flores MVC, et al. Runx3 Is Required for Hematopoietic Development in Zebrafish. *Dev Dyn.* 2003;228(3):323-336.
- Wang CQ, Krishnan V, Tay LS, et al. Disruption of Runx1 and Runx3 leads to bone marrow failure and leukemia predisposition due to transcriptional and DNA repair defects. *Cell Rep.* 2014;8(3):767-782.
- Bruijn M De, Dzierzak E. Runx transcription factors in the development and function of the definitive hematopoietic system. *Blood.* 2017;129(15):2061-2070.
- Wang CQ, Motoda L, Satake M, et al. Runx3 deficiency results in myeloproliferative disorder in aged mice. *Blood.* 2013;122(4):562-567.
- Finck R, Zunder ER, Gonzalez VD, et al. Palladium-based mass tag cell barcoding with a doublet-filtering scheme and single-cell deconvolution algorithm. *Nat Protoc.* 2015;10(2):316-333.
- Tusi BK, Wolock SL, Weinreb C, et al. Population snapshots predict early haematopoietic and erythroid hierarchies. *Nature.* 2018;555(7694):54-60.
- Wahlestedt M, Norddahl GL, Sten G, et al. An epigenetic component of hematopoietic stem cell aging amenable to reprogramming into a young state. *Blood.* 2013;121(21):4257-4264.
- Ren R, Ocampo A, Liu GH, Izpisua Belmonte JC. Regulation of Stem Cell Aging by Metabolism and Epigenetics. *Cell Metab.* 2017;26(3):460-474.
- Waki T, Tamura G, Sato M, Terashima M, Nishizuka S, Motoyama T. Promoter methylation status of DAP-kinase and RUNX3 genes in neoplastic and non-neoplastic gastric epithelia. *Cancer Sci.* 2003;94(4):360-364.
- Gunnell A, Webb HM, Wood CD, et al. RUNX super-enhancer control through the Notch pathway by Epstein-Barr virus transcription factors regulates B cell growth. *Nucleic Acids Res.* 2016;44(10):4636-4650.
- Mabuchi M, Kataoka H, Miura Y, et al. Tumor suppressor, AT motif binding factor 1 (ATBF1), translocates to the nucleus with runt domain transcription factor 3 (RUNX3) in response to TGF- $\beta$  signal transduction. *Biochem Biophys Res Commun.* 2010;398(2):321-325.
- Ogawa S, Satake M, Ikuta K. Physical and functional interactions between STAT5 and Runx transcription factors. *J Biochem.* 2008;143(5):695-709.
- Torquati A, O'Rear L, Longobardi L, Spagnoli A, Richards WO, Daniel Beauchamp R. RUNX3 inhibits cell proliferation and induces apoptosis by reinstating transforming growth factor beta responsiveness in esophageal adenocarcinoma cells. *Surgery.* 2004;136(2):310-316.
- Chen X, Deng Y, Shi Y, et al. Loss of expression rather than cytoplasmic mislocalization of RUNX3 predicts worse outcome in non-small cell lung cancer. *Oncol Lett.* 2018;15(4):5043-5055.
- Kuvarina ON, Herglotz J, Kolodziej S, et al. RUNX1 represses the erythroid gene expression program during megakaryocytic differentiation. *Blood.* 2015;125(23):3570-3579.
- Bagger FO, Kinalis S, Rapin N. BloodSpot: a database of healthy and malignant haematopoiesis updated with purified and single cell mRNA sequencing profiles. *Nucleic Acids Res.* 2019;47(D1):D881-D885.
- Goodnough LT, Schrier SL. Evaluation and Management of Anemia in the Elderly. *Am J Hematol.* 2014;89(1):88-96.
- Krishnan V, Ito Y. RUNX3 loss turns on the dark side of TGF- $\beta$  signaling. *Oncoscience.* 2017;4(11-12):156-157.
- Mendelson A, Frenette PS. Hematopoietic stem cell niche maintenance during homeostasis and regeneration. *Nat Med.* 2014;20(8):833-846.
- Waki T, Tamura G, Sato M, Motoyama T. Age-related methylation of tumor suppressor and tumor-related genes: An analysis of autopsy samples. *Oncogene.* 2003;22(26):4128-4133.
- Li B, Ding L, Yang C, et al. Characterization of transcription factor networks involved in umbilical cord blood CD34+ stem cells-derived erythropoiesis. *PLoS One.* 2014;9(9):e107133.